Simulation of reactive transport of uranium(VI) in groundwater with variable chemical conditions

Gary P. Curtis,[1] James A. Davis,[1] and David L. Naftz[2]

Received 21 January 2005; revised 19 November 2005; accepted 3 January 2006; published 7 April 2006.

[1] The reactive transport of U(VI) in a shallow alluvial aquifer beneath a former U(VI) mill located near Naturita, CO, was simulated using a surface complexation model (SCM) to describe U(VI) adsorption. The groundwater had variable U(VI) concentrations (0.01–20 μM), variable alkalinity (2.5–18 meq/L), and a nearly constant pH equal to 7.1. U(VI) K_D values decreased with increasing U(VI) and alkalinity, and these parameters were more important than sediment variability in controlling K_D values. Reactive transport simulations were fit to the observed U(VI) and alkalinity by varying the concentration of U(VI) and alkalinity in recharge at the source area. Simulated K_D values varied temporally and spatially because of the differential transport of U(VI) and alkalinity and the nonlinearity of U(VI) adsorption. The model also simulated the observed U(VI) tailing, which would not be expected from a constant K_D model. The simulated U(VI) concentrations were sensitive to the recharge flux because of the increased flux of U(VI) to the aquifer. The geochemical behavior of U(VI) was most sensitive to the alkalinity and was relatively insensitive to pH.

Citation: Curtis, G. P., J. A. Davis, and D. L. Naftz (2006), Simulation of reactive transport of uranium(VI) in groundwater with variable chemical conditions, *Water Resour. Res.*, *42*, W04404, doi:10.1029/2005WR003979.

1. Introduction

[2] Uranium in groundwater aquifers is a contaminant of concern at many U.S. federal government sites where it has been stored in poorly designed facilities or where it has been leached from U mill tailings [*USDOE*, 1996; *Abdelouas et al.*, 1999; *Crowley and Ahearne*, 2002]. A critical aspect of assessing the risk of contaminated groundwater and performance of potential remedies at many uranium-contaminated sites is estimating the migration of U in groundwater. Uranium occurs in the environment predominantly as U(IV) in reducing systems and U(VI) in oxic systems. In reducing environments, U(IV) forms insoluble phases and therefore is relatively immobile [*Langmuir*, 1997]. In oxic environments, U(VI) forms moderately soluble solid phases [*Grenthe et al.*, 1992] such that at concentrations less than approximately 30 μM, the mobility of U(VI) can be controlled by adsorption reactions at near neutral pH values [*Davis et al.*, 2004].

[3] Adsorption of U(VI) in oxic waters is sensitive to pH and carbonate concentration and therefore to the partial pressure of CO_2. Adsorption is generally low at low pH values and increases with increasing pH usually in the pH range of 4 to 6 [*Hsi and Langmuir*, 1985; *Waite et al.*, 1994; *Pabalan et al.*, 1998; *Davis et al.*, 2002]. In the pH range of approximately 7–10, U(VI) is strongly adsorbed in the absence of dissolved CO_2 [*Hsi and Langmuir*, 1985; *Prikryl et al.*, 2001] but in the presence of dissolved CO_2, the formation of aqueous U(VI)-carbonate complexes can cause adsorption to be negligible [*Hsi and Langmuir*, 1985; *Waite et al.*, 1994; *Davis et al.*, 2004; *Wazne et al.*, 2003]. Adsorption could also be reduced by the formation of $CaUO_2(CO_3)_3^{-2}$ and $Ca_2UO_2(CO_3)_3^0$ species that can be the dominant U(VI) aqueous species in many groundwaters [*Bernhard et al.*, 2001; *Brooks et al.*, 2003; *Fox et al.*, 2006].

[4] A simple approach to describe U(VI) adsorption by a sediment is to use a constant distribution coefficient defined by

$$K_D = \frac{U_{ADS}}{U_{AQU}} \quad (1)$$

where K_D is the distribution coefficient (mL/g), U_{ADS} is the adsorbed U(VI) concentration (mol/g), and U_{AQU} is the total dissolved U(VI) concentration in groundwater (mol/mL). However, U(VI) K_D values can vary by five orders of magnitude over the pH range from 6 to 9 and by 4 orders of magnitude at pH 8 as the partial pressure of CO_2 gas increases from its value in air to 0.01 atm [*Davis et al.*, 2004]. Therefore, simulations with a constant K_D can introduce significant error into transport simulations because the constant K_D approach does not account for temporally and spatially variable geochemical conditions that can be present within a contamination plume or for extensive tailing caused by the nonlinear adsorption isotherms [*Reardon*, 1981; *Kohler et al.*, 1996; *Bethke and Brady*, 2000; *Glynn*, 2003; *Zhu*, 2003].

[5] Surface complexation models (SCM) can account for the effect of variable solution chemistry on adsorption and for a finite quantity of adsorption sites and have been used to model U(VI) adsorption in many laboratory studies [*Hsi and Langmuir*, 1985; *Waite et al.*, 1994; *Pabalan et al.*, 1998; *McKinley et al.*, 1995; *Turner and Sassman*, 1996;

[1] U.S. Geological Survey, Menlo Park, California, USA.
[2] U.S. Geological Survey, West Valley City, Utah, USA.

Kohler et al., 1996; *Villalobos et al.*, 2001; *Davis et al.*, 2004]. In the SCM approach, adsorption is postulated to occur on specific surface sites, e.g.,

$$>SOH + UO_2^{2+} + H_2O \quad = \quad >SOUO_2OH + 2H^+ \qquad (2)$$

where UO_2^{+2} is the free uranyl ion in solution, >SOH is a protonated surface site and $>SOUO_2OH$ is a possible uranyl surface complex. This approach makes it possible to describe binding to a finite number of surface sites (which leads to nonlinear isotherms) and to simulate pH-dependent adsorption processes. Moreover, adsorption reactions can be readily coupled to extensive databases of solution speciation reactions as exemplified by the formation of the aqueous uranium tricarbonato complex, i.e.:

$$UO_2^{2+} + 3\ CO_3^{-2} \quad = \quad UO_2(CO_3)_3^{-4} \qquad (3)$$

When considered together, equations (2) and (3) illustrate that >SOH and CO_3^{-2} compete for UO_2^{+2}; in instances where the CO_3^{-2} concentration is large the formation of mobile U(VI)-carbonate complexes is favored.

[6] One approach for applying the SCM approach to sediments uses published SCMs for well-characterized surfaces coupled with detailed soil characterization studies to determine the quantity of each reactive surface in the soil and then assembles an SCM for the sediment from its basic components [*Davis et al.*, 1998; *Westall et al.*, 1998]. However, *Davis et al.* [2004] had limited success when this approach was used to model U(VI) adsorption by aquifer sand obtained at the site described in this study. Four significant sources of uncertainty were identified: (1) estimation of surface site-types and surface area abundances, even for well characterized sediments, (2) a lack of fundamental data on the effects of competitive adsorption of common groundwater solutes, (3) a lack of fundamental data on the effects of common groundwater solutes on surface charge and potentials, and (4) inconsistencies that could result when combining previously published SCMs that use different electrical double layer formulations. To reduce these uncertainties, a semi-mechanistic SCM was calibrated to measured adsorption data [*Davis et al.*, 2004]. In this approach, adsorption is postulated to occur on generic surface sites that represent average properties of the sediment surfaces rather than specific mineral surfaces. Model parameters are calibrated to adsorption data for postulated reaction stoichiometries and different model formulations are selected based on simplicity and goodness of fit [*Davis et al.*, 2002, 1998; *Waite et al.*, 2000]. An advantage of this approach is that the electrical double layer is not considered explicitly; adsorption reaction stoichiometry and binding constants are derived by fitting the macroscopic dependence of adsorption as a function of pH. This is important because of the difficulty in quantifying electrical field and charge at the mineral-water interface in mixtures of mineral phases with associated surface coatings.

[7] The SCM approach has only been used in a few instances to describe adsorption in field-scale reactive transport modeling studies. These studies include cases involving the transport of molybdate [*Stollenwerk*, 1998], zinc [*Kent et al.*, 2000], and phosphate [*Parkhurst et al.*, 2003], all of which were conducted at the USGS Cape Cod field site. Reactive transport simulations for U(VI) transport have been limited by a lack of site-specific data [*Zhu et al.*, 2001; *Zhu and Burden*, 2001].

[8] The purpose of this work, together with a set of companion papers [*Davis et al.*, 2004; *Kohler et al.*, 2004; *Curtis et al.*, 2004], is to demonstrate the application of the semi-mechanistic SCM approach for modeling the adsorption and reactive transport of U(VI) in an alluvial aquifer at a former uranium ore-processing mill near Naturita, CO. The SCM for U(VI) adsorption was determined in laboratory batch studies with Naturita aquifer background sediments (NABS) [*Davis et al.*, 2004], and the model gave good predictions of U(VI) adsorption by contaminated sediments [*Kohler et al.*, 2004] and in *in situ* studies with NABS [*Curtis et al.*, 2004]. The outline of the remainder of this paper is as follows: (1) describe the significant geochemical characteristics of the field site, (2) evaluate the factors that control adsorption and transport of U(VI) in the field, (3) compare reactive transport simulations using the SCM approach with the field observations, and (4) illustrate the sensitivity of the simulated U(VI) concentration to key model parameters.

2. Site Characterization

2.1. Site Description

[9] The former uranium mill site is approximately 3 km northwest of the town of Naturita, CO along the San Miguel River in southwestern Colorado (Figure 1). The ore mill processed uranium and vanadium ores at the site intermittently during the 1930s and beginning in 1939 almost continuously until the mill was shut down in 1958 [*USDOE*, 2003]. From 1961 until 1963, a uranium upgrader that produced uranium concentrates that were further processed elsewhere was operated at the site. Uranium and vanadium were extracted from the ore by salt roasting followed by carbonate leaching in percolation tanks. Carbonate leach tails were slurried to the western half of the site farthest (200 meters) from the San Miguel River and closest to CO highway 141 and were later collected and leached with sulfuric acid. Acid leach tails were deposited closer to the river. Between 1977 and 1979, the mill tailings were removed from the site for reprocessing and between 1996 and 1998 the contaminated soils below the former tailings and mill were excavated and transported offsite. The extent of the excavation was determined by ^{226}Ra measurements and as a result, soils were excavated to as deep as the water table below most of the former mill yard and tailings [*USDOE*, 2003]. This excavated area was backfilled with clean sediments, but as illustrated in the cross-section in Figure 1, the excavation lowered the ground surface elevation by several meters.

2.2. Hydrogeology

[10] The Naturita area is semi-arid; the average annual precipitation is 30 centimeters and the vegetation is primarily grasses and sagebrush except near the river where cottonwoods are common. Historical aerial photos indicate that there was little vegetation in the mill yard or on the tailings pile. Contaminated groundwater at the Naturita site occurs in the thin alluvial deposits of the San Miguel River floodplain. The aquifer is bounded by outcrops of fine-grained shale (the Brushy Basin member) on the west near

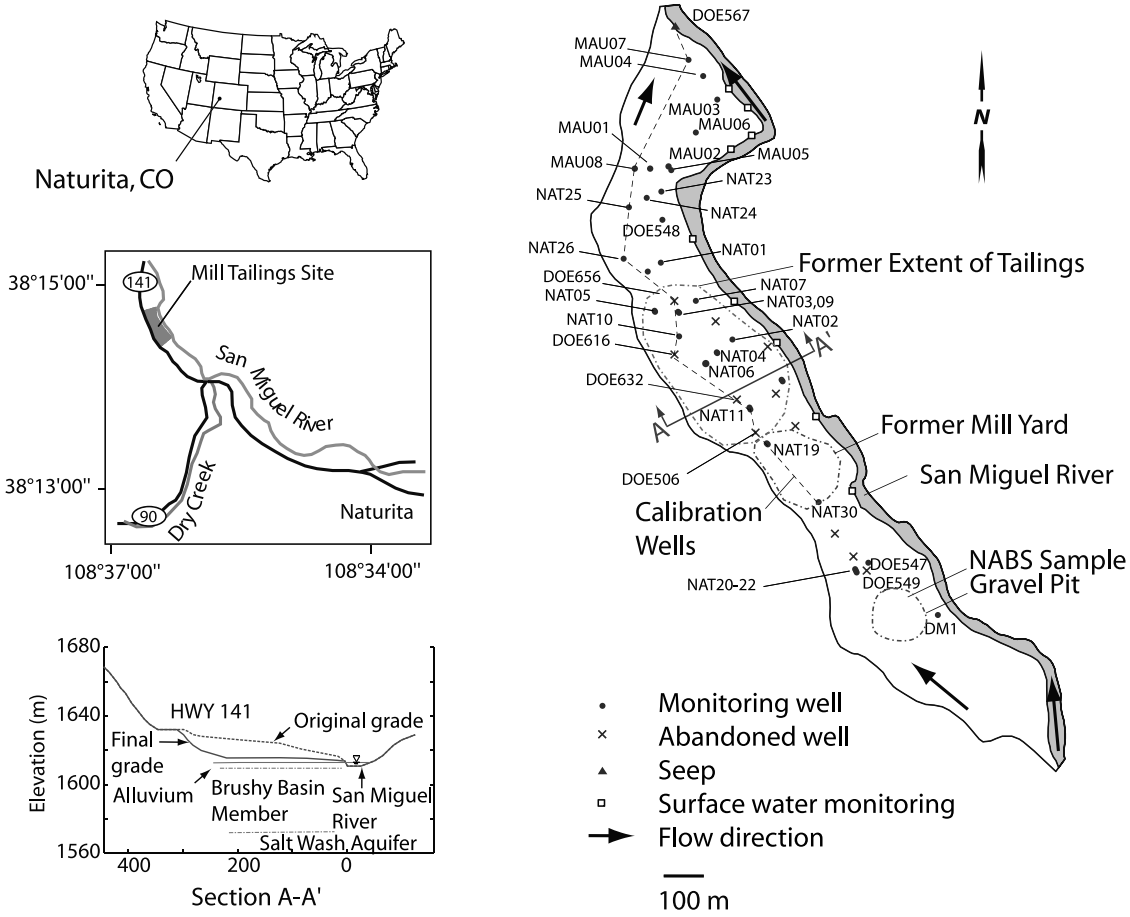

Figure 1. Naturita field site showing the location of the former mill yard, the extent of the tailings the monitoring wells and a cross section at the former tailing pile. The dashed line connects wells used for model calibration.

highway 141 and to the east of the San Miguel River (Figure 1). The aquifer is recharged by the river to the southeast of the site and discharges into the river north of the site. The average saturated thickness is 1.8 m when the river is at low-flow conditions. The alluvial aquifer consists of sand, gravel and cobbles and the mineralogy consists of primarily quartz with lesser amounts of detrital feldspars, carbonates, magnetite, and fine clay-size materials [*Davis et al.*, 2004]. The unsaturated zone ranged from approximately 2 to 8 m thick prior to the removal of contaminated soils but the thickness averaged 2.5 m after the excavation was backfilled in 1998.

[11] The alluvial aquifer is separated from an underlying, moderately permeable confined sandstone aquifer (the Salt Wash aquifer) by the Brushy Basin Member, which is approximately 30 m thick. A well in the Salt Wash aquifer was artesian prior to being abandoned in 1996 indicating the potential for upward transport. However, the deep groundwaters had an average chloride (Cl) concentration of 20 mM, which was 200 times larger than Cl in background alluvial wells indicating minimal upward flow. The average U(VI) concentration in the Salt Wash aquifer was 0.16 μM.

2.3. Geochemical Characterization

[12] Figure 1 shows the location of the former mill yard, the extent of the former tailings pile, and all of the monitoring wells at the site. Between 1986 and 1997, DOE installed 12 wells in the alluvial aquifer. All of these wells except DOE547 and DOE548 were abandoned during surface remediation. In 1998 and 1999, the USGS installed wells at 39 new locations including some clusters of multilevel wells. High concentrations of uranium were measured in the groundwater below and downgradient of the former tailings pile. Either water used to process the U ore and mill tailings or precipitation that leached U from the deposited tailings could have transported U to the groundwater.

2.3.1. Dissolved Concentrations

[13] Groundwater samples were collected from the 12 DOE wells between 1986 and 1997 by DOE [*USDOE*, 1998] and from the 52 USGS wells and DOE547 and DOE548 between 1998 and 2001 by USGS. In this pooled data set, 474 water samples had a complete set of analytical results and 469 samples had charge balance errors less than 15 percent and were used in the following analyses. The observed alkalinity, pH, U(VI) and Cl concentrations are summarized in Table 1. Most of the pH values ranged from 6.5 to 7.5, and the median pH was 7.06. The U(VI) concentration ranged from background values of 0.01 μM to about 10 μM although 2 samples had concentrations greater than 20 μM. Most of the alkalinity values ranged from 2.5 to approximately 12 meq/L although 5 samples

Table 1. Summary of Observed pH, U(VI), Alkalinity, and Chloride in Naturita Groundwater, 1986–2001 in 469 Samples and K_D Calculated From the Semimechanistic SCM and the Groundwater Composition for Each Groundwater Analysis

Percentile	pH	Dissolved U(VI), μM	Alkalinity, meq/L	Chloride, mM	K_D, mL/g
Minimum	6.54	0.0084	2.47	0.06	0.17
2.5	6.75	0.030	3.21	0.13	0.64
17	6.90	0.16	4.77	0.29	1.19
Median	7.06	2.78	6.79	1.24	1.24
83	7.23	5.25	8.11	2.99	2.03
97.5	7.48	9.87	11.2	13.6	6.57
Maximum	7.71	21.8	18.0	24.1	12.9

collected between 1986 and 1992 had alkalinity values between 12 and 18 meq/L. The samples with the highest alkalinity did not coincide with the samples with highest U(VI), but in general, the two concentrations were correlated. The high concentrations of Cl in about 10 percent of the samples most likely resulted from the salt roasting process used to extract U from the ore. The concentrations of the major ions, pH, alkalinity and U(VI) in the multilevel wells did not show any vertical variability. Additional details on the geochemical and hydrogeologic characteristics of the site are summarized by *Davis and Curtis* [2003].

[14] Elevated concentrations of U(VI), alkalinity, and chloride were observed below and downgradient of the former uranium mill tailings and the concentration of each species was generally lower near the San Miguel River and higher near the highway (Figure 2). In February 2000, the average U(VI) concentration in the wells upgradient of the former facilities (e.g. DM1, DOE547, and NAT20-22) was 0.02 μM, and a peak concentration of 10 μM was observed at NAT26; most of the impacted groundwater had U(VI) concentrations between 2 and 6 μM. Similar trends were observed for other sampling rounds.

[15] Figure 2b suggests that the pH was up to 0.8 pH units higher near the river when compared with values farther from the river. However, this pattern of pH values did not persist over multiple sampling sets as was observed for the U(VI) and alkalinity patterns.

[16] The observed alkalinity had a somewhat similar spatial pattern as U(VI) but the range in concentrations was smaller (Figure 2c). The alkalinity values ranged from approximately 4.7 meq/L near DOE547 to peak values of 12 meq/L at NAT26. As in the case of U(VI), the zone of elevated alkalinity occurred widely across the site. The figure also suggests that high alkalinity concentrations extend farther downgradient than the uranium concentration. Several samples collected in 2000 and 2001 from DOE547 had alkalinity values in the range of 2.5 to 3 meq/L; these smaller alkalinity values are consistent with the loss of CO_2 and precipitation of calcite from standing water in gravel pits upgradient of DOE547 that have been significantly expanded since 1998.

[17] The geochemistry of the groundwater from the upgradient wells DM1, DOE547, and NAT20-22 was significantly different from that in the San Miguel River. The wells had pH values that were approximately one pH unit less than the pH of 8.3 observed in the river. Similarly, the groundwater had an average alkalinity of 4.7 meq/L whereas the alkalinity in the San Miguel River varied seasonally between 1.3 and 2.6 meq/L. The decrease in the pH and the increase in alkalinity for the surface water to groundwater transition are consistent with biological activity. Other studies have reported mild reducing conditions and active microbial populations in groundwaters near tree roots possibly because of microbial degradation of root exudates [*Lee et al.*, 2000; *Godsy et al.*, 2003]. In the Naturita aquifer, this reducing activity is assumed to be limited to the hyporheic zone including the root zone of cottonwood trees near the river because water samples from DM1, which is only 10m from the river, were similar to those from DOE547 which is ~120m away from the river.

[18] The groundwaters at the Naturita site are generally not in equilibrium with respect to redox conditions. This is indicated by the co-occurrence of dissolved O_2 and Fe^{+2} in many samples, which is not expected under equilibrium conditions at near neutral pH values [*Langmuir*, 1997]. Nitrate concentrations in 45 samples collected between 1986 and 1992 ranged from 8 to 730 μM and had an average concentration of 120 μM. Although these samples were collected at different times than the samples analyzed for Fe, the long-term trends suggest that the two species co-occurred in some wells, which is not expected under equilibrium conditions.

2.3.2. Speciation Calculations

[19] Aqueous speciation calculations were performed using the thermodynamic data summarized previously [*Davis et al.*, 2004]. These thermodynamic data included data for the $Ca_2UO_2(CO_3)^0_{3(aq)}$ and $CaUO_2(CO_3)^{2-}_2$ aqueous species [*Kalmykov and Choppin*, 2000; *Bernhard et al.*, 2001] and these two species accounted for more than 95% of the total U(VI) in solution in each of the 469 water samples. Saturation indices (SI) were computed to assess if several potentially important minerals could be controlling U(VI) transport. The computed SI values were found to be

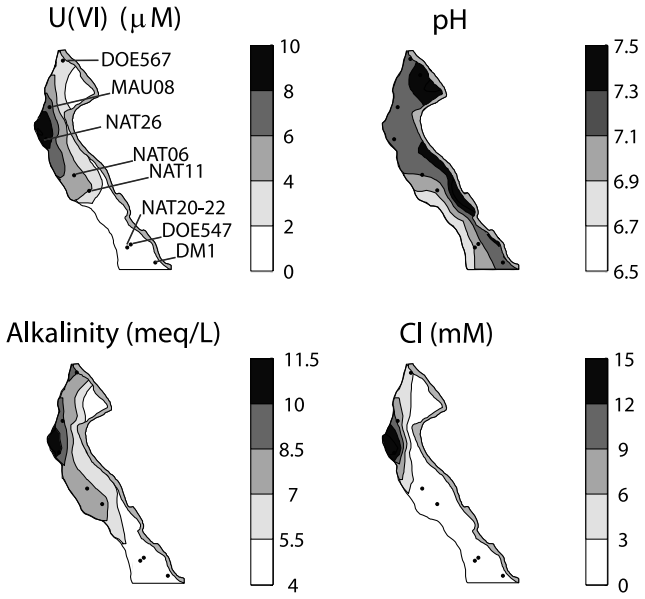

Figure 2. Observed concentrations of (a) U(VI), (b) pH, (c) alkalinity, and (d) Cl in groundwater samples collected in February 2000.

Table 2. NABS Surface Complexation Model[a]

Reaction	Symbol[b]	Log K[c]
$>SSOH + UO_2^{2+} = >SSOUO_2^+ + H^+$	K_{SS}	6.80
$>SOH + UO_2^{2+} = >SOUO_2^+ + H^+$	K_S	5.82
$>WOH + UO_2^{2+} = >WOUO_2^+ + H^+$	K_W	2.57
$>SSOH + UO_2^{2+} + H_2O = >SSOUO_2OH + 2H^+$	K_{SSOH}	−0.67
$>SOH + UO_2^{2+} + H_2O = >SOUO_2OH + 2H^+$	K_{SOH}	−2.08
$>WOH + UO_2^{2+} + H_2O = >WOUO_2OH + 2H^+$	K_{WOH}	−5.32

[a]From *Davis et al.* [2004]. The total site concentration was 1.92×10^{-6} sites/g. The fraction of weak sites (>WOH) was 0.9989, the fraction of strong sites (>SOH) was 0.001, and the fraction of very strong sites (>SSOH) was 0.0001.

[b]The symbols are used in Figures 10 and 11 to identify different reaction properties.

[c]Log of apparent binding constant.

below saturation for uranophane ($Ca(UO_2)_2SiO_3(OH)_2$; SI < −7.7), soddyite ($(UO_2)_2SiO_2 2H_2O$; SI < −3.5), schoepite ($(UO_2(OH)_2H_2O$; SI < −5) and rutherfordine (UO_2CO_3; SI < −4.4). These SI values are consistent with detailed characterization of contaminated sediments from NAT06 and MAU03 that did not identify any U(VI) phases [*Davis et al.*, 2004]. Calcite SI values generally ranged from −0.25 to 0.35 suggesting that the groundwaters were in equilibrium with calcite, which is present in the sediments. Computed pCO_2 values ranged from 0.0024 to 0.14 atm.

[20] Speciation calculations were also performed to evaluate the stability of the U(IV) phases uraninite and U_3O_8. The calculations assumed that the Fe(III)/Fe(II) couple was at equilibrium with the U(VI)/U(IV) couple and that the Fe(III) activity was controlled by the presence of either ferrihydrite or goethite. The U(IV) phases were below saturation (SI < −5) if equilibrated with ferrihydrite and near saturation (−2 < SI < 2) if equilibrated with goethite illustrating the large uncertainty resulting from the two model assumptions. Rather than relying on these model calculations, *Kohler et al.* [2004] extracted U from freshly collected sediments from near NAT25 under an inert atmosphere and demonstrated that U(IV) phases were not important at that location.

2.3.3. Uranium Adsorption

[21] In the absence of separate U phases, adsorption is probably the most significant factor that reduces U(VI) mobility in the alluvial aquifer. Batch adsorption experiments were conducted using Naturita aquifer background sediments (NABS) that were collected from a gravel pit located upgradient of well DOE547 [*Davis et al.*, 2004]. The batch experimental conditions encompassed the range of geochemical conditions observed in the field and a semimechanistic SCM was fit to the adsorption data using the geochemical optimization program FITEQL [*Herbelin and Westall*, 1999]. The SCM consists of 6 reactions and 3 different site-types that are listed in Table 2. The three site-types are described as very strong (>SSOH), strong (>SOH), and weak (>WOH) sites, corresponding to their relative U(VI) binding strength (Table 2). Multiple site-types are commonly used in formulating SCMs and approximate the nonlinear isotherms commonly observed for cation adsorption on well-characterized metal oxides [*Dzombak and Morel*, 1990]. Postulating multiple site-types was also important for simulating peak tailing of U(VI) in laboratory columns packed with quartz [*Kohler et al.*, 1996]. *Davis et al.* [2004] illustrated that observed and modeled K_D values at constant pH and alkalinity decreased by a factor of approximately 3 as U(VI) concentration increased from 0.03 μM to 10 μM indicating that the adsorption isotherm is moderately nonlinear. The semimechanistic SCM does not include an electrical double layer term and assumes that the adsorption occurs by U(VI) binding to generic sites that represent average surface chemical properties of the sediment.

[22] Figure 3 shows a comparison of model-predicted K_D values with observations obtained for uncontaminated NABS samples that were suspended in wells with contaminated groundwater [*Curtis et al.*, 2004] and for contaminated sediments for both field conditions and laboratory conditions [*Kohler et al.*, 2004]. The results for the uncontaminated NABS samples (Figure 3a) show that the measured K_D values ranged from 0.55 mL/g to 12.5 mL/g corresponding to a factor of 22 and the model-predicted values agreed with measured values within a factor of 2.2. For the contaminated sediments under field conditions, the K_D values for all samples except those from MAU03 and MAU04 ranged by a factor of 15 and a good agreement between the measured and model-predicted values was found (Figure 3b). For samples from MAU03 and MAU04, it has been postulated that a U(IV) phase forms because of localized reducing conditions, possibly related to nearby cottonwood tree roots. In comparison, K_D values

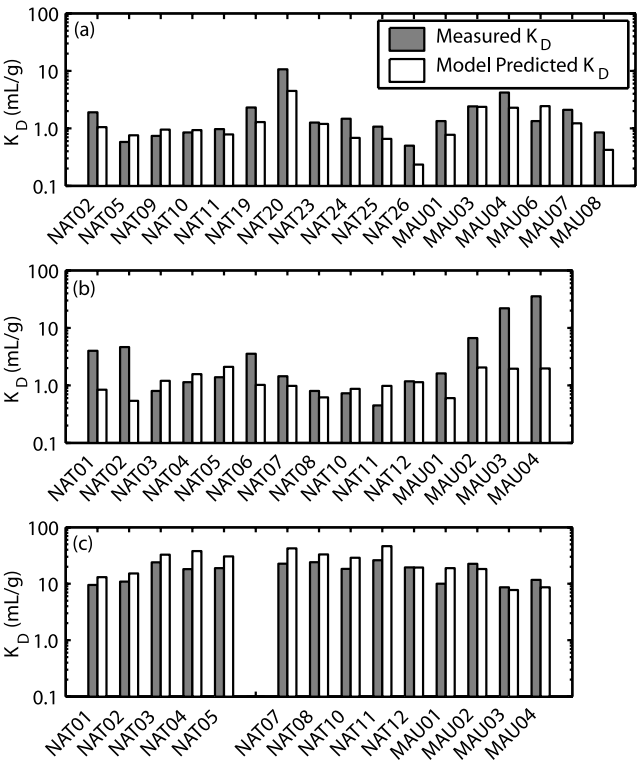

Figure 3. Comparison of measured and model-predicted K_D values for (a) NABS samples suspended in 2″ wells at the field site [*Curtis et al.*, 2004], (b) contaminated sediments in equilibrium with in situ groundwater [*Kohler et al.*, 2004], and (c) contaminated sediments in equilibrium with artificial groundwater and laboratory air [*Kohler et al.*, 2004].

shown in Figure 3c for the 14 contaminated sediments that were equilibrated with an artificial groundwater with a nearly constant composition varied by only a factor of 3. Taken together, the K_D values for a single sediment (NABS) equilibrated with 17 different groundwater compositions varied considerably more than was observed for 14 different sediments equilibrated with a single artificial groundwater. These results demonstrate that at this site, spatially variable U(VI) and alkalinity were more important than variable sediment composition in determining uranium K_D values. Similar observations were made for the effect of pH on Zn adsorption in the presence of sediments from a glacial outwash aquifer on Cape Cod [*Davis et al.*, 1998].

3. Groundwater Flow and Nonreactive Transport

3.1. Conceptual Model

[23] The shallow alluvial aquifer was approximated as a two-dimensional areal aquifer. No-flow boundary conditions were assumed along contacts with the Brushy Basin Member which occurs on the western border of the aquifer, on the eastern border of the San Miguel River, and at the bottom of the alluvial aquifer. Pressure transducers installed in the aquifer and in the river demonstrated that the aquifer was in good hydraulic contact with the river. Stream discharge ranged from a base-flow of approximately 1 m^3/s to peak flows of 30 to 110 m^3/s; low-flow conditions were generally constant for approximately 8 to 9 months of the year.

[24] A spatially and temporally uniform recharge rate of 5.5×10^{-3} m/y (~2% of annual precipitation) was assumed in all of the simulations. The recharge conveyed contaminated water into the aquifer as described below but it did not significantly affect the simulated potentiometric surface. Although evapotranspiration may have been important for the riparian woodland areas along the stream banks, it was not included in the flow model because of the good hydraulic contact between the river and the aquifer. Evaporation resulting from capillary rise was not included because the unsaturated zone was moderately thick until 1997.

[25] Transport simulations used an assumed porosity of 0.2 because the cobbles, which were assumed to have no porosity, accounted for approximately 50% of the solid aquifer volume [*Davis et al.*, 2004]. A longitudinal dispersivity of 3 m was used which is about half of the value for sites of similar scale [*Gelhar et al.*, 1992]. This relatively small amount of macrodispersion was used because excessive macrodispersion can over-predict mixing which could drive many reactions that affect the adsorption and transport of U(VI). One simulation with a dispersivity of 1 m gave nearly identical results (not shown) as was observed for a dispersivity of 3 m.

3.2. Model Calibration: Estimates of Hydraulic Conductivity

[26] The hydraulic conductivity (K_X) of the aquifer was initially estimated from slug tests. Slug tests were performed on 10 wells distributed across the site and each well was tested 3 to 5 times. The harmonic mean K_X was 2.2×10^{-4} m/s and the results ranged by a factor of 3. There was no spatial trend for the K_X values and therefore, a single value was considered in the transport simulations described below.

[27] K_X was also estimated by simultaneously fitting a nonreactive solute transport model to both the observed Cl plume and to tritium-helium ($^3H/^3He$) age dating results. The chloride plume was assumed to have originated from the salt roasting facilities in the mill yard and from the mill tailings. Other sources of Cl including road salt and vertically upward flow of water from the Salt Wash Aquifer were discounted because the U(VI) and SO_4 concentrations in the Cl plume were also high. It is unlikely that road salt would have contained high SO_4 and U(VI) and the Salt Wash Aquifer had U(VI) values that were 2000 times smaller than the observed U(VI) at NAT26.

[28] The $^3H/^3He$ ages reflect the residence time in the aquifer, which is controlled primarily by the K_X value and the recharge rate. Groundwater age can therefore be used to estimate hydraulic parameters [*Reilly et al.*, 1994; *Portniaguine and Solomon*, 1998]. In this method, ^3H in groundwater originating primarily from atmospheric testing is measured along with its daughter, ^3He, and the ratio of the two values is related to the groundwater age [*Solomon and Cook*, 2000]. The measured age can be biased by loss of ^3He to the unsaturated zone. However, when the transport is nearly horizontal, this potential loss is controlled by the vertical dispersivity [*Solomon and Cook*, 2000], which is generally small in many unconfined aquifers [*Burnett and Frind*, 1987]. Consequently, vertical dispersive mixing is not considered to seriously affect the estimated groundwater ages [*Solomon and Cook*, 2000].

[29] An integral part of the parameter estimation was to approximate the Cl concentration in the recharge water. It was assumed that Cl was initially released at the site in 1939 when the salt roaster started continuous operation. It was also assumed that the Cl source was present until the contaminated soils were excavated from the unsaturated zone beginning in 1994. This long duration is postulated to be the result of leaching of Cl from stored tailings by precipitation followed by transport through the unsaturated zone and it is consistent with the presence of contaminated soils at the site. The simulated Cl transport was calibrated to Cl data collected between 1986 and 2001 at 11 locations. These locations included wells NAT19, DOE506, NAT11, DOE616, NAT10, DOE656, NAT26, NAT25, MAU08, and MAU07, which are highlighted on Figure 1. One sample collected in 2001 from a seep present at low river stage (DOE567) was also included in the calibration set. The locations were selected for the length of record and because they are approximately on a flow path that is far from the river.

[30] Groundwater flow in the alluvial aquifer was simulated using a steady-state flow model using MODFLOW [*Harbaugh and McDonald*, 1996]. The river was simulated in the flow model using the MODFLOW river package. Nonreactive transport was simulated with MT3DMS [*Zheng and Wang*, 1999] and the $^3H/^3He$ age was also simulated with MT3DMS using the method described by [*Goode*, 1996].

[31] The model was calibrated to the observed data using UCODE [*Poeter and Hill*, 1998] to estimate the K_X value and the Cl concentration of contaminated recharge water. Other parameters used in the flow model are listed in Table 3. The contaminated recharge water was assumed to have been present in an area defined by the former U mill

Table 3. Summary of Nonreactive Transport Model Parameters

Parameter	Units	Value	Source
Hydraulic conductivity (K_X)	m/s	1.0×10^{-4}	calibrated
Chloride	M	0.12	calibrated
Recharge rate	m/y	5.5×10^{-4}	assumed
Porosity	m^3/m^3	0.2	assumed
Dispersivity	m	3	assumed

and tailing piles as shown in Figure 1. Figure 4 shows that a reasonable calibration was achieved for a K_X value of 1×10^{-4} m/s and a Cl concentration in the recharge water of 0.12M. The calibrated model fit all of the observed Cl values at the 11 calibration wells with the possible exception of well DOE616 as shown in Figure 4d. This well was located near the former salt roaster, which could explain why higher Cl values were observed in that area. Figure 4l shows that the simulated groundwater ages agree well with the observed values. Although the calibration may not be unique, the simultaneous fit of the Cl and ^{3}H/He results lends support to the model.

[32] The K_X value determined from the Cl and groundwater age simulations is 2.2 times smaller than the harmonic mean K_X of 2.2×10^{-4} m/s obtained from the slug tests. The slug tests give a direct measure of the hydraulic conductivity whereas the K_X value estimated from transport models depend on an assumed porosity. If a larger porosity had been assumed in the calibration, larger K_X values would have been estimated from the model calibration. An unrealistically large porosity of greater than 0.5 would have been required for the Cl simulations to match the observed Cl data with a K_X value from the slug tests. The slug test results could be higher because they can be impacted by small-scale heterogeneities in the aquifer. Although the Cl transport could have been impacted by possible connected zones of high permeability, this effect would probably not be apparent in the observed data because the Cl plume reached the river by 1998 and possibly earlier.

[33] Figure 5 illustrates the simulated Cl plume for a K_X value of 1 $x10^{-4}$ m/s and flow paths calculated with MODPATH [*Pollock*, 1994]. The shape of the plume, including the location of the maximum Cl concentration, agrees well with the observed Cl plume (Figure 2d). The flow path lines show that the groundwater flow is approximately parallel to the river due to the no-flow boundary condition along the western edge of the aquifer and the small recharge rate. The flow pathlines also show extensive coupling between the river and the aquifer and that a long, thin plume develops between MAU08 and DOE567. This elongated plume develops because flow converges in this region because of the extensive groundwater-surface water interactions east of MAU08 to MAU07. The velocity near MAU08 was approximately twice as large as upgradient near NAT10.

4. Reactive Transport Modeling

[34] Reactive transport simulations were fitted to the observed distribution of U(VI) at the Naturita site using the independently determined K_X and the independently determined SCM for NABS [*Davis et al.*, 2004]. This section describes: (1) the effect of variable chemical conditions at the Naturita site on U(VI) transport, (2) application of the reactive transport model to simulate the current

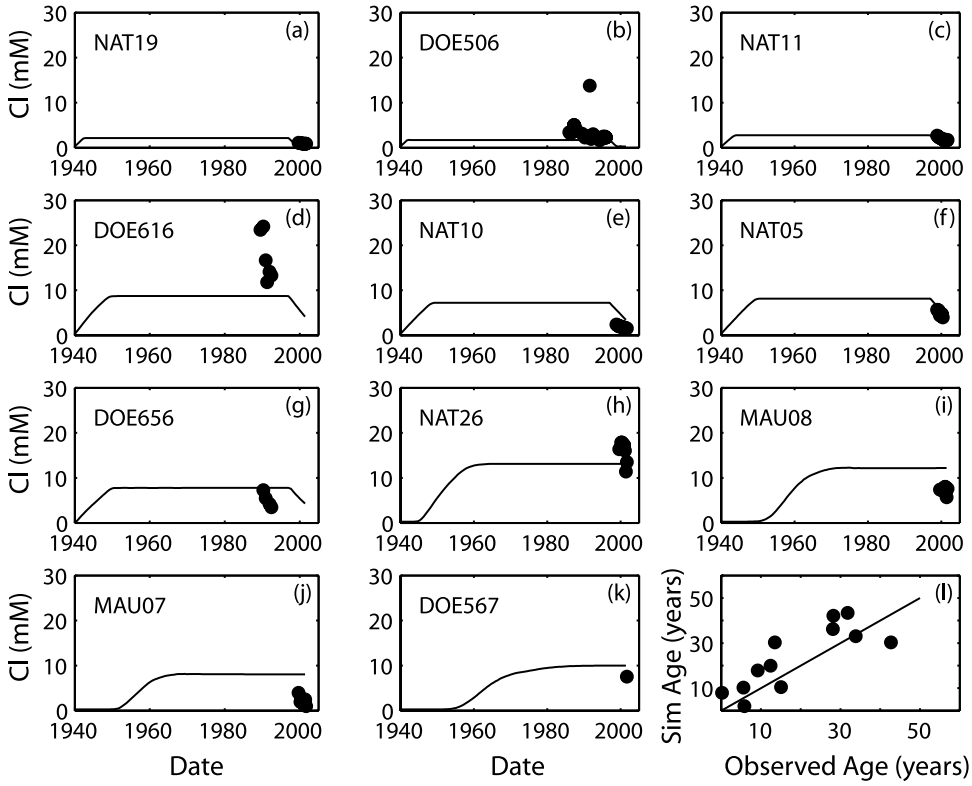

Figure 4. Chloride calibration results for a 59-year source at the former mill site and tailings pile (Figures 4a–4k) and comparison between observed and simulated groundwater ages (Figure 4l).

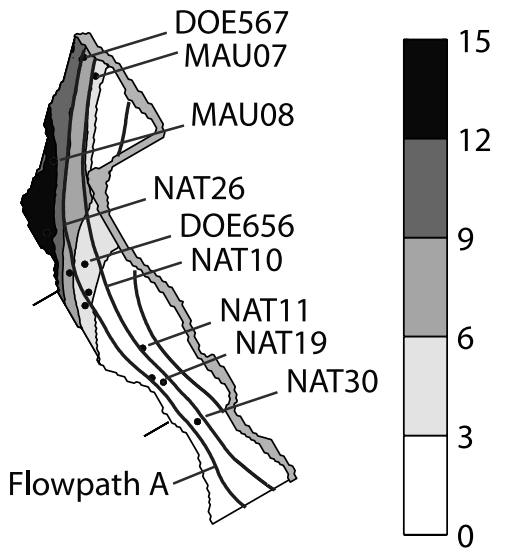

Figure 5. Simulated chloride plume (mM) and groundwater flow path lines obtained using the calibrated flow and transport model. Tick marks on the left boundary indicate the extent of the source term.

existing conditions, and (3) results of a sensitivity analysis that evaluated the effects of SCM parameters, flow and transport parameters, and background concentrations on U(VI) transport. Simulations were performed using RATEQ [*Curtis*, 2005], which couples reactive transport to MODFLOW and MT3DMS.

4.1. Effect of Variable Chemical Conditions on U(VI) Adsorption and Transport

[35] As shown in Figure 3, the observed variable chemical conditions had a larger effect than sediment variability on measured K_D values. One-dimensional transport simulations were conducted to evaluate which of the three parameters, alkalinity, pH, or U(VI) concentration, was most significant in determining U(VI) mobility. Simulations were conducted by introducing long pulses of a U(VI) bearing solution that displaced water that had a pH of 7.1, an alkalinity of 2.5 meq/L and a low U(VI) concentration of 5×10^{-12}M. The injected high-U(VI) solution used constant and median values for 2 parameters (such as pH and alkalinity) and the observed range of values for the third parameter (U(VI)). The values used in the simulations are summarized in Table 1 and all simulations assumed that the Ca concentration was in equilibrium with calcite. Although this approach does not consider the correlation between U(VI) and alkalinity, these hypothetical simulations provide some insight into the effects of each of the parameters on U(VI) mobility.

[36] Figure 6a shows the breakthrough of a U(VI) pulse (2.78 μM) for pH values that ranged from 6.54 to 7.71. Simulated U(VI) breakthrough ($C/C_O = 0.5$) occurs between 7.4 and 8.5 pore volumes. Later breakthrough was associated with higher pH values although the simulations were relatively insensitive to pH. Figure 6b shows the breakthrough of a U(VI) pulse for U(VI) concentrations that ranged from 0.0084 to 21.8 μM. These breakthrough curves cluster into two groups. The first cluster breaks through between 4.9 and 7.5 pore volumes and is associated with U(VI) concentrations equal to or greater than the median U(VI) concentration (2.78 μM). The second cluster breaks through at approximately 11.5 pore volumes and is associated with U(VI) concentrations of 0.16 μM and smaller. The larger retardation at smaller U(VI) concentrations occurs because the U(VI) adsorption isotherm on NABS is nonlinear [*Davis et al.*, 2004]. For U(VI) concentrations greater than 0.16 μM, the very strong sites are nearly completely saturated but account for less that 15% of total adsorbed U(VI) and consequently U(VI) migration is controlled primarily by adsorption on the strong and weak sites. Conversely, at concentrations smaller than 0.16 μM, the very strong sites dominate adsorption causing greater retardation.

[37] Figure 6c shows that the observed variability of alkalinity has the largest effect on U(VI) front migration. U(VI) breakthrough occurred between 3.9 and 15.7 pore volumes and retardation increased with decreasing alkalinity. The simulations show that U(VI) transport is particu-

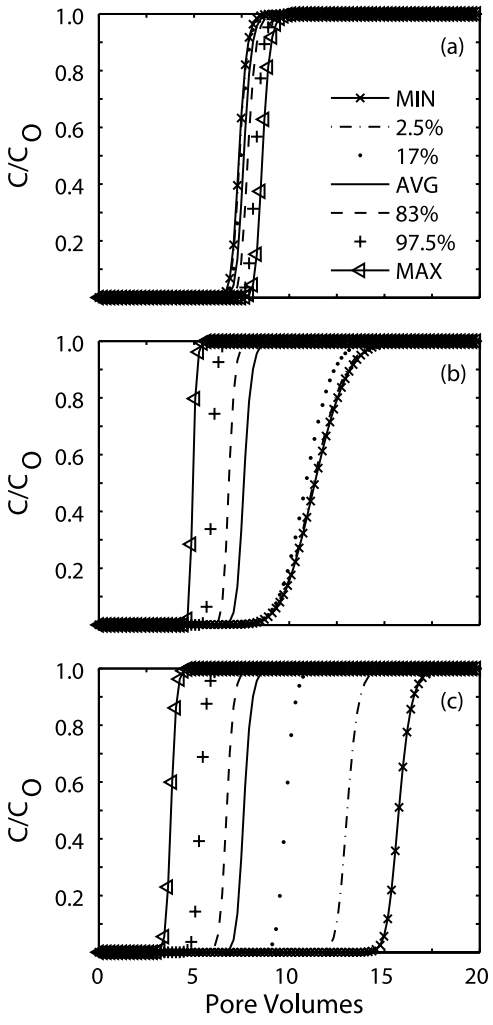

Figure 6. Simulated breakthrough created by a step change in inlet boundary conditions. The boundary conditions were (a) variable pH, median U(VI) concentration, and median alkalinity, (b) median pH, variable U(VI), and median alkalinity, and (c) median pH, median U(VI), and variable alkalinity. See Table 1 for specific concentration values.

Table 4. Composition of Uncontaminated and Contaminated Groundwaters

Constituent	Units	Uncontaminated Source Water[a]	Contaminated Source Water
Cl^-	mM	0.089	118[b]
U(VI)	μM	0.061	97.7[b]
Alkalinity	meq/L	4.87	79.4[b]
pH	SU	7.07	7.30[c]
Ca^{+2}	mM	2.32[d]	0.273[d]
Na^+	mM	0.32[e]	197[e]
$>WOH_T$	mM	37.9	NA[f]
$>SOH_T$	mM	0.03795	NA
$>SSOH_T$	mM	0.003795	NA

[a]Average composition of upgradient wells. Uncontaminated water was used for the initial and boundary conditions in the aquifer.
[b]Cl, U(VI), and alkalinity were obtained by model calibration.
[c]Assumed value.
[d]Ca^{+2} concentration was calculated from the solubility of calcite that was assumed to be present in excess.
[e]Na^+ concentration was computed from the charge balance.
[f]Not applicable.

larly sensitive to alkalinity at low alkalinity values. For example, the average background alkalinity is 4.7 meq/L, which is close to the alkalinity at the 17th percentile of 4.77 meq/L. Breakthrough at this latter alkalinity occurred at 10 pore volumes whereas a U(VI) pulse in water with the minimum alkalinity (2.5 meq/L) broke through at 15.7 pore volumes. Overall, the simulations suggest that the variability of alkalinity at the site has a larger effect on U(VI) migration than either U(VI) concentration or pH. In addition, because alkalinity and U(VI) were correlated in the field, the overall range in mobility is larger than that implied in Figure 6 which considered each variable independently.

4.2. Conceptual Field-Scale Reactive Transport Model

[38] The conceptual reactive transport model couples the flow and transport model described above for Cl transport with geochemical speciation and adsorption model described by *Davis et al.* [2004]. The aqueous complexation reactions used in the transport simulations included the $Ca_2UO_2(CO_3)_3^{-2}$ and $CaUO_2(CO_3)_2^o$ aqueous species [*Kalmykov and Choppin*, 2000; *Bernhard et al.*, 2001] which were the dominant species in solution.

[39] Adsorption reactions were simulated using the SCM calibrated to U(VI) adsorption by NABS in laboratory experiments [*Davis et al.*, 2004]. The total concentration of the adsorption sites was calculated from an average surface area of the aquifer sediments of 12.4 m^2/g [*Kohler et al.*, 2004] and a total surface site density of 1.92 μmoles/m^2 [*Davis et al.*, 2004]. These values, together with an assumed porosity of 0.2 and adjusting for the observation that the NABS sample represented 15% of the aquifer sediments [*Davis et al.*, 2004] gave a total adsorption site concentration of 3.79×10^{-2} mol sites per liter of groundwater.

[40] The simulations assumed equilibrium with respect to calcite because the sediments contained calcite and the groundwater was nearly in equilibrium with calcite. Calcite solubility controls the concentrations of Ca and CO_3, both of which significantly impact the aqueous speciation of U(VI). Although U(VI) can be incorporated into the calcite structure to some extent [*Reeder et al.*, 2001; *Kelly et al.*, 2003], extractions of contaminated sediments indicated this was a small affect for the Naturita site [*Kohler et al.*, 2004].

[41] The field-scale simulations assumed local equilibrium for the adsorption reactions and separate simulations described elsewhere [*Davis and Curtis*, 2003] demonstrated that this was a reasonable assumption because adsorption approached equilibrium in approximately three days. The simulations ignored all redox reactions. The initial geochemical conditions used in the simulations were set equal to the average composition observed in the upgradient wells DOE547 and NAT20-22 and are listed in Table 4. It was also assumed that the composition of the recharge water from the river could be approximated by the background groundwater composition. This assumption was supported by observations that the geochemical changes that occurred as river water infiltrated into the aquifer were complete in a relatively small spatial scale near the river as discussed above.

4.3. Field Transport Modeling

4.3.1. Model Calibration

[42] It was assumed that spatially uniform recharge water derived from precipitation had elevated U(VI) and alkalinity concentrations in the same source zone used to calibrate the flow model in section 3. This zone included the former mill yard and the tailings pile and the simulated recharge in this zone was contaminated for the 58 years that the mill yard and the tailings were present at the site. The extent and duration of the source term is consistent with the area that was excavated, in most instances to as deep as the water table, during the soil remediation work performed between 1996 and 1998 [*USDOE*, 2003]. The depth and lateral extent of that excavation was determined by radiological analysis, primarily ^{226}Ra, of the contaminated vadose zone sediments.

[43] The reactive transport model was calibrated to the existing site data using UCODE [*Poeter and Hill*, 1998] by optimizing the U(VI) concentration and the alkalinity of the recharge water in the source area. The recharge water had a fixed pH of 7.3, was assumed to be in equilibrium with calcite, and contained NaCl as determined from the flow model calibration (section 3.2). The observed and simulated U(VI) and alkalinity concentrations were normalized by the recent maximum observed concentrations of U(VI) (10 μM) and alkalinity (12.1 meq/L) so that each variable ranged between zero and one. This normalization ensured that the two different concentrations were weighted nearly equally. The calibration did not vary the SCM parameters determined in the batch experiments [*Davis et al.*, 2004] or K_X, which was determined independently as described above. A single source concentration was used for the entire source area because when separate source terms were included for the mill yard and the tailings area the model was difficult to calibrate because of the covariance among the source concentrations.

[44] Figure 7 illustrates the final calibration results for U(VI) and alkalinity at each of the calibration wells. For each well, there is good agreement between the simulated and observed alkalinity values. The largest consistent difference between the simulated and observed alkalinity occurred at well DOE656 where measured values ranged from 16 to 21 meq/L, whereas the simulated value was

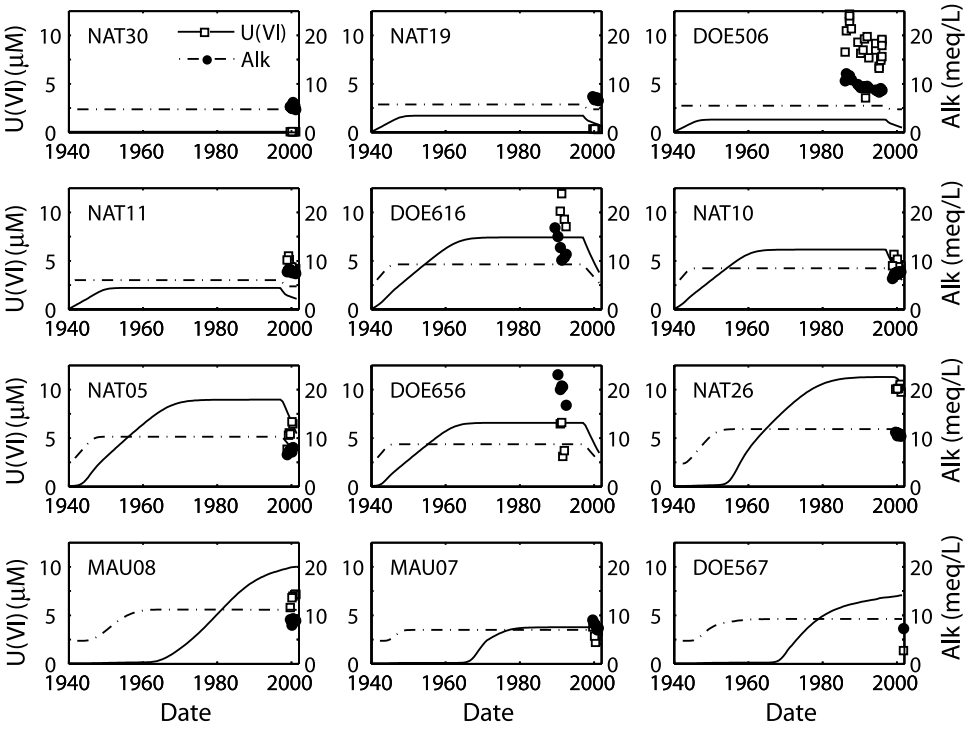

Figure 7. Reactive transport model calibration results. Each plot shows the observed dissolved U(VI) (open squares), simulated dissolved U(VI) (solid lines), observed alkalinity (solid circles), and simulated alkalinity (dash-dotted lines).

9.5 meq/L. For all other wells, the agreement between the simulated and measured values is better, with the average residual equal to 2.8 meq/L. The fit to the dissolved U(VI) data is also generally very good and the average residual was 2 μM. The largest, consistent difference between the simulated and observed U(VI) concentrations was for well DOE506, which was located at the downstream border of the mill yard. Possibly U(VI) was high at this location because of a more highly concentrated source in the mill yard. In the final calibration simulations, the alkalinity in the recharge water was 79 meq/L and the U(VI) concentration was 98 μM (Table 4). These estimated concentrations are approximately a factor of 6 to 9 times larger than the maximum concentrations observed in the aquifer, which is plausible. This comparison, however, depends on the assumed recharge rate of 5.5×10^{-3} m/y. For recharge rates less than 2×10^{-2} m/y, nearly identical simulation results were obtained when the solute fluxes, defined by the product of concentration times the recharge rate, were constant.

4.3.2. Spatial and Temporal Simulation Results

[45] Figure 8 shows the simulated distributions of U(VI) and alkalinity in 1967 and 2000. The simulated U(VI) plume for 2000 reproduces the main features of the observed U(VI) plume shown in Figure 2. Not only does the simulated peak concentration agree well with the observations (Figure 7), but the general shape of the plume is also reproduced. This agreement includes the generally lower concentrations near the San Miguel River as well as the long narrow plume that extends downgradient of NAT26. The good fit of the simulations to the observations was obtained using an average surface area of 12.4 m^2/g to calculate the total adsorption site concentration and the measured surface areas ranged by a factor of only approximately 4 [*Kohler et al.*, 2004]. Preliminary simulations that accounted for the spatial variability of the surface areas showed that the variable surface had no significant effect of U(VI) transport [*Curtis*, 2005], probably because the measured surface areas ranged by only a factor of four.

[46] In the case of the alkalinity, the general shape of the simulated plume also agrees with the observed plume, although not as well as in the case of U(VI). The largest difference between the observed and simulated alkalinity values was that the simulated values were smaller than the observations in the region between NAT10 and NAT19. These differences are also apparent in Figure 7 for wells NAT11 and NAT19 where the simulated alkalinity values in 2000 are approximately 2 meq/L smaller that the observed values. This difference is visually emphasized in Figure 8 because of the large distance between NAT10 and NAT19. The alkalinity simulation is generally similar to the Cl simulations shown in Figure 4 suggesting that alkalinity is transported nearly conservatively. The simulated pH (not shown) was practically constant because of the buffering from calcite.

[47] Figure 8 also shows a subtle difference between the simulated highest alkalinity and U(VI) plumes near the western model boundary downgradient of NAT26 in 1967. The simulated alkalinity is adjacent to the western boundary and extends all the way to the river. In contrast, for U(VI), the plume extends downgradient of NAT26 as a long, thin lobe with a clear region with low U(VI) concentrations adjacent to the western boundary. This difference results because U(VI) is retarded relative to alkalinity.

[48] Figure 8 also shows the temporal and spatial evolution of dissolved U(VI) and alkalinity and the simulated K_D

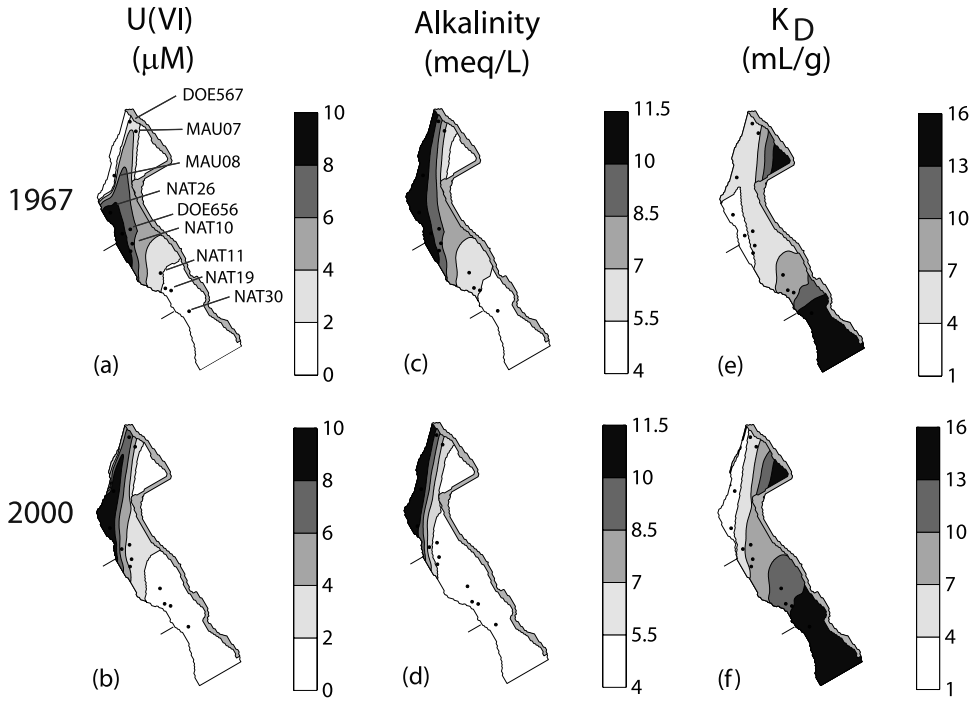

Figure 8. Simulated spatial distribution of dissolved U(VI) concentration, alkalinity, and simulated K_D values in 1967 and 2000. Tick marks on the left boundaries indicate the extent of the source term.

values. The simulated K_D values were computed from equation 1 and then converting to the units of mL/g. With increasing time, the U(VI) and alkalinity plumes increase in size and the maximum concentration of each species also increased. These increases in U(VI) and alkalinity caused the K_D values to decrease because of both the nonlinearity of the isotherm and the formation of dissolved U(VI) carbonate complexes. Moreover, the K_D values change with increasing time because of the changes in geochemical conditions. A comparison of the 1967 and 2000 simulations show that the region with K_D values smaller than 4 mL/g expanded into an area downgradient of the source zone. In contrast, in the upgradient region, the K_D values generally increased between 1967 and 2000 as the groundwater slowly returns to background conditions. This increase in K_D value causes the significant tailing observed for U(VI) that would not be simulated using a constant K_D transport model.

[49] The simulated adsorbed U(VI), dissolved U(VI) and alkalinity along flow path A (Figure 5) from the upgradient border of the former mill yard to the San Miguel River near DOE567 are shown in (Figure 9a). In the source area, which encompasses the first 500 m of the flow path, the simulated alkalinity returned to background conditions whereas the simulated aqueous and adsorbed U(VI) had a pronounced tail. This tail results because of both the nonlinear adsorption isotherm and the variable alkalinity concentrations that combine to change the K_D value by a factor of 4.

[50] For the surface species, adsorption on the weak and strong sites is nearly comparable (Figures 9b and 9c). Near the upgradient boundary of the former mill yard where the U(VI) concentration is relatively small, the adsorbed concentration on the weak sites is only 50% of the strong site adsorbed concentration. Downgradient where the dissolved U(VI) and alkalinity were at their maximum values the weak site adsorbed concentration is equal to approximately 80% of the strong site. These changing percentages result because adsorption on the strong sites between 400 and 800 m is probably affected by the limited concentration (38 μM) of strong sites. This is even more important for the very strong sites that have a total concentration of only 3.8 μM and a maximum simulated adsorbed concentration of 2.2 μM. Although the very strong sites are not important at high U(VI) concentration, they account for approximately one third of the total adsorption in the upgradient zone. For each of the three site-types, the surface uranyl cation is the dominant species compared to the corresponding neutral species. The effect of charge balance error resulting from the immobile cation was considered in separate simulations and was found to be negligible [*Davis and Curtis*, 2003]. For the weak site, the neutral species accounts for approximately 16% of the adsorption to that site (Figure 9b), but for the very strong site the neutral species accounts for approximately 40% of the adsorption to that site (Figure 9d). The neutral species is relatively more important when the U(VI) and alkalinity values are small.

4.4. Sensitivity Analysis

[51] First-order sensitivity analyses were calculated for the simulated U(VI) concentrations. The scaled sensitivities [*Poeter and Hill*, 1998] were defined by

$$SS_i = \frac{\partial Y}{\partial b_i} b_i \tag{4}$$

where SS_i is the scaled sensitivity, Y is the simulated quantity, and b_i is the i'th parameter value. The scaling normalizes the sensitivity by the parameter values so that

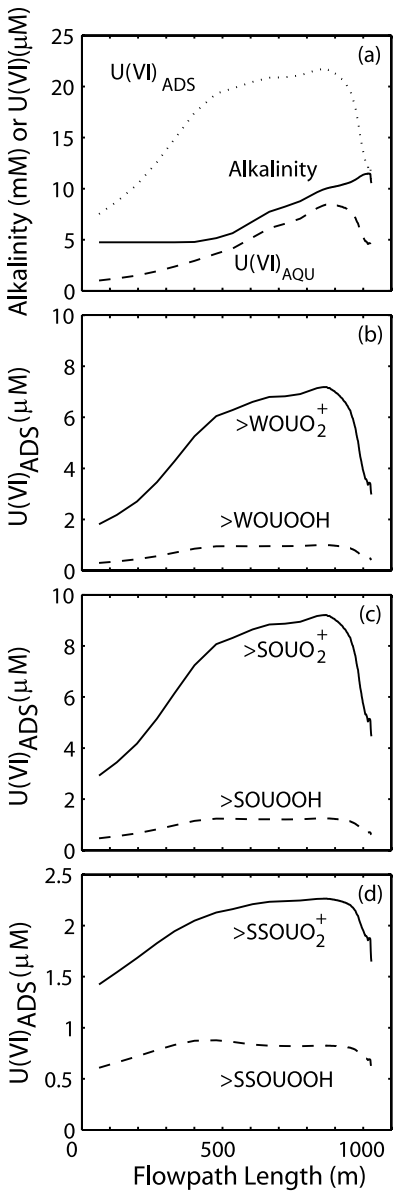

Figure 9. Simulated concentrations of (a) alkalinity, dissolved and total adsorbed U(VI), and U(VI) adsorbed by (b) weak site, (c) strong sites, and (d) very strong sites. The simulated concentrations were taken along flow path A for the year 2001.

the sensitivities with respect to widely varying parameter values can be easily compared. Equation 4 was approximated by first-order finite differences and for consistency, the parameters were increased by 0.1 log units.

[52] The scaled sensitivities were calculated for both the calibration parameters and parameters that were otherwise held constant including the adsorption model parameters and flow model parameters such as the recharge rate and the porosity. The sensitivities of the simulated U(VI) concentration along flow path A to the flow model parameters are shown in Figure 10a. The sensitivity to K_X is less than zero up to 800 meters and greater than zero beyond 800 meters because the increased K_X values causes the U(VI) to migrate faster. Thus, concentrations in the downgradient area increased while concentrations in the upgradient area decreased because of increased velocities. The sensitivity to the recharge rate is uniformly greater than zero because the increase in the recharge rate increased the fluxes of U(VI) and alkalinity from the contaminated source and only slightly increased the groundwater velocity. Although both porosity and K_X were used in computing velocities, the porosity also affects the adsorption site concentrations, which were expressed in units of moles of sites per liter of groundwater. Consequently, the U(VI) concentrations were more sensitive to the porosity than K_X. The simulations were relatively insensitive to dispersivity because a small dispersivity was assumed to minimize the effect of dispersion on reactions.

[53] The sensitivity of the simulated U(VI) to the U(VI) concentration, alkalinity and pH values in both the contaminated recharge and the background waters are shown in Figures 10b and 10c, respectively. Not surprisingly, the U(VI) concentration in the plume was sensitive to the U(VI) concentration in the recharge water but was insensitive to the low U(VI) concentration in the background water. Positive sensitivities were observed for the alkalinity in both the recharge and background waters reflecting the tendency for U(VI) to be less adsorbed and more mobile in the presence of the increased alkalinity.

[54] The sensitivites to the SCM parameters are shown in Figures 10d, 10e, and 10f for the weak, strong, and very strong sites, respectively. For the weak site, the sensitivity to the equilibrium constant for the formation of the surface cation is nearly equal to that for the total weak site concentration. This occurs because the surface cation was

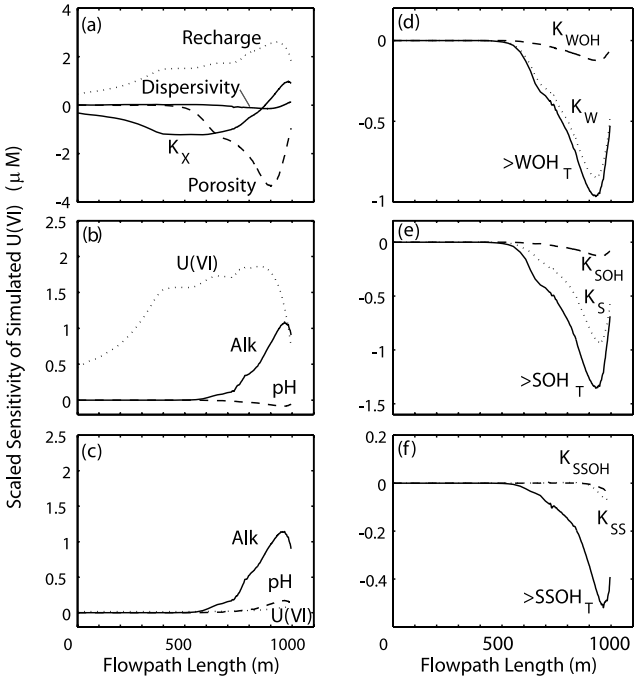

Figure 10. Scaled sensitivities of simulated U(VI) concentration along flow path A for (a) flow and transport model parameters, (b) concentrations in the source water, (c) concentrations in the background water, and SCM parameter for the (d) weak site, (e) strong site, and (f) very strong site.

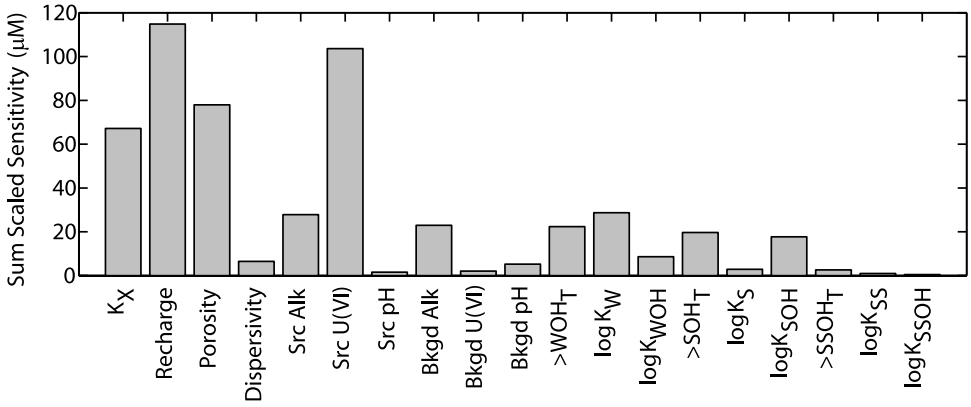

Figure 11. Scaled sensitivity of simulated U(VI) concentration summed over the entire model domain for the year 2001. Concentrations in the source area are denoted by the prefix "Src," and concentrations in the background area are denoted by the prefix "Bkgd." See Table 2 for other abbreviations.

the dominant surface species and the total site coverage was relatively low. Under these conditions, the equilibrium constants (K_W) and the total site densities ($>WOH_T$,) are highly covariant. Similar results were found for the strong site (Figure 10d). This was not observed for the very strong site because the surface is nearly fully saturated. Finally, taken together, the sensitivities shown in Figure 10 demonstrate that all of the sensitivities vary spatially and therefore vary temporally because of U(VI) and alkalinity migration.

[55] Figure 11 shows the sum of the absolute scaled sensitivity over the entire computational domain for each parameter considered in the sensitivity calculations. This figure shows that the model is most sensitive to the recharge rate. However, the model is nearly equally sensitive to the U(VI) concentration in the source water suggesting that primary reason that the model is sensitive to the recharge rate is that the recharge rate increases the flux of U(VI) into the aquifer. The model is also sensitive to K_X. In general, the sensitivities for the SCM parameters were approximately 25% or less of that for K_X. This smaller sensitivity results, in part, because when a parameter for one of the sites was increased resulting in increased adsorption to that site, the effect was compensated for by decreased adsorption to the other two sites. The total sensitivity of the simulated U(VI) concentration to the SCM parameters can be approximated as the sum of the sensitivity of only $>WOH_T$, $>SOH_T$ and $>SSOH_T$ because of the covariance among the SCM parameters. This estimated total sensitivity to the SCM parameters was 43 μM, which is about 64% of the K_X value.

[56] The sensitivity values resulting from this simplified analysis primarily illustrates how each parameter affects the simulated U(VI) concentration. However, the sensitivity analysis alone does not indicate which parameters are most important in controlling the uncertainty of the simulations. The importance of a parameter has been related to the product of the parameter sensitivity times the uncertainty of that parameter [*Tiedeman et al.*, 2004]. Thus, parameters having relatively small sensitivity values and large uncertainties can be equally important as parameters that have large sensitivities and small uncertainties. This paper demonstrates that SCM can do a good job simulating U(VI) transport, even though the sensitivity and uncertainty of the simulations might be dominated by K_X.

5. Concluding Remarks

[57] The reactive transport simulations presented above illustrate that the semi-mechanistic SCM approach for simulating adsorption accounts for the spatially and temporally variable chemical conditions and their affect on the U(VI) retardation. In plumes with chemical gradients, the spatial distribution of K_D values can be quite complex and be characterized by significant spatial character. These complex spatial patterns also evolve temporally because of transport processes. The temporal and spatial distribution of the K_D values is particularly important when considered in view of the common practice in performance assessments where K_D values are typically represented by statistical distributions. Performance assessment modelers must recognize not only that variable chemical conditions can cause a range of effective K_D values to be observed, but also that the spatial distribution of K_D values within that range is not likely to be a random function or a normal distribution.

[58] Although the reactive transport model including the semi-mechanistic SCM described here was successful at a specific site, the modeling approach could be useful for simulating the transport of U(VI) at other field sites with chemically variable conditions. This modeling approach is a compromise between the simple constant K_D approach and the most complex SCMs which attempt to account for each of many minerals present in a sediment and possibly the electrical double layer properties of these sediments. The semi-mechanistic approach is based on the premise that although natural soils and sediments consist of a mixture of many minerals, the surface chemistry of these minerals is dominated by coatings and adsorption to these surfaces can be described with a relatively small set of reactions and mass action expressions. The semi-mechanistic modeling approach can be applied in instances where transport is controlled by adsorption, and it does not require an overly burdensome program of data collection [*Kent et al.*, 2000; *Davis et al.*, 2004] when compared with data required to formulate and calibrate a groundwater flow and transport model. In addition, relative to the constant

K_D approach, the SCM approach could reduce adsorption model uncertainty such that the total uncertainty is dominated by the hydraulic conductivity.

[59] The use of the semi-mechanistic SCM, while limited in its description of the detailed chemical mechanisms, has the important advantage that it couples extensive databases for aqueous speciation reactions with mass action expression for adsorption reactions. The modeling approach is therefore capable of accounting for the effects of variable chemical conditions on reactive transport involving adsorption reactions. This was important in the Naturita case because U(VI) was retarded whereas HCO_3, the primary species included in solution alkalinity for the field conditions, probably migrated nearly conservatively. This difference in mobility for U(VI) and HCO_3 causes K_D values to vary temporally and spatially in the aquifer. Despite these complexities, reactive transport simulations that included the semi-mechanistic SCM and used a reasonable approximation of the source term could be fitted to the U(VI) and alkalinity observed in the field.

[60] **Acknowledgments.** This work was supported by the U.S. Nuclear Regulatory Commission (interagency agreement RES-97-009) and the U.S. Geological Survey Toxic Substances Hydrology program. We thank Geoff Freethey for constructing the initial groundwater flow model and Chris Wilkowske, Ryan Rowland, and Walt Holmes for assistance in the field. We also thank Neil Plummer, Ed Busenberg, and Julian Wayland for conducting the tritium-helium age dating analyses. The use of trade names in this paper is for identification purposes only and does not constitute endorsement of the U.S. Geological Survey. We thank Hedeff Essaid and Douglas Kent, Robert Bowman, James Hunt, and two anonymous reviewers for comments on the manuscript.

References

Abdelouas, A., W. Lutze, and H. E. Nuttall (1999), Uranium contamination in the subsurface: Characterization and remediation, in *Uranium: Mineralogy, Geochemistry and the Environment, Rev. Mineral. Ser.*, vol. 38, pp. 433–473, Mineral. Soc. of Am., Washington, D. C.

Bernhard, G., G. Geipel, T. Reich, V. Brendler, S. Amayri, and H. Nitsche (2001), Uranyl(VI) carbonate complex formation: Validation of the $Ca_2UO_2(CO_3)_3$ (aq) species, *Radiochim. Acta*, *89*, 511–518.

Bethke, C. M., and P. V. Brady (2000), How the K_d approach undermines group water cleanup, *Ground Water*, *38*(3), 435–443.

Brooks, S. C., J. K. Fredrickson, S. L. Carroll, D. W. Kennedy, J. M. Zachara, A. E. Plymale, S. D. Kelly, K. M. Kemner, and S. Fendorf (2003), Inhibition of bacterial U (VI) reduction by calcium, *Environ. Sci. Technol.*, *37*(9), 1850–1858.

Burnett, R. D., and E. O. Frind (1987), Simulation of contaminant transport in three dimensions: 2. Dimensionality effects, *Water Resour. Res.*, *23*(4), 695–705.

Crowley, K. D., and J. F. Ahearne (2002), Managing the environmental legacy of US. nuclear weapons production, *Am. Sci.*, *90*, 514–523.

Curtis, G. P. (2005), Documentation and applications of the reactive geochemical transport model RATEQ, Draft report for comment, *Rep. NUREG/CR-6871*, 97 pp., U. S. Nucl. Regul. Commiss., Rockville, Md. (Available at http://www.nrc.gov/reading-rm/doc-collections/nuregs/contract/cr6871/index.html)

Curtis, G. P., P. Fox, M. Kohler, and J. A. Davis (2004), Comparison of field uranium K_D values with a laboratory surface complexation model, *Appl. Geochem.*, *19*(10), 1643–1653.

Davis, J. A., and G. P. Curtis (2003), Application of surface complexation modeling to describe uranium (VI) adsorption and retardation at the uranium mill tailings site at Naturita, Colorado, 223 pp., U.S. Nucl. Regul. Commiss., Rockville, Md. (Available at http://www.nrc.gov/reading-rm/doc-collections/nuregs/contract/cr6820/)

Davis, J. A., J. A. Coston, D. B. Kent, and C. C. Fuller (1998), Application of the surface complexation concept to complex mineral assemblages, *Environ. Sci. Technol.*, *32*(19), 2820–2828.

Davis, J. A., T. E. Payne, and T. D. Waite (2002), Simulating the pH and pCO_2 dependence of uranium (VI) adsorption by a weathered schist with surface complexation models, in *Geochemistry of Soil Radionuclides*, pp. 61–86, Soil Sci. Soc. of Am., Madison, Wis.

Davis, J. A., D. E. Meece, M. Kohler, and G. P. Curtis (2004), Approaches to surface complexation modeling of uranium (VI) adsorption on aquifer sediments, *Geochim. Cosmochim. Acta*, *68*(18), 3621–3641.

Dzombak, D. A., and F. M. M. Morel (1990), *Surface Complexation Modeling: Hydrous Ferric Oxide*, John Wiley, Hoboken, N. J.

Fox, P., J. A. Davis, and J. M. Zachara (2006), The effect of calcium on aqueous uranium(VI) speciation and adsorption to ferrihydrite and quartz, *Geochim. Cosmochim. Acta*, *70*, 1379–1387.

Gelhar, L. W., C. Welty, and K. R. Rehfeldt (1992), A critical review of data on field-scale dispersion in aquifers, *Water Resour. Res.*, *28*(7), 1955–1974.

Glynn, P. D. (2003), Modeling Np and Pu transport with a surface complexation model and spatially variant sorption capacities; implications for reactive transport modeling and performance assessments of nuclear waste disposal sites; reactive transport modeling in the geosciences, *Comput. Geosci.*, *29*(3), 331–349.

Godsy, E. M., E. Warren, and V. V. Paganelli (2003), The role of microbial reductive decholorination of TCE at a phytoremediation site, *Int. J. Phytoremediation*, *5*(1), 73–88.

Goode, D. J. (1996), Direct simulation of groundwater age, *Water Resour. Res.*, *32*(2), 289–296.

Grenthe, I., J. Fuger, R. J. M. Konings, R. J. Lemire, A. B. Muller, C. Nguyen-Trung, and H. Wanner (1992), *Chemical Thermodynamics of Uranium*, 715 pp., Elsevier, New York.

Harbaugh, A. W., M. G. McDonald (1996), Programmer's documentation for MODFLOW-96, an update to the U.S. Geological Survey modular finite-difference ground-water flow model, *U.S. Geol. Surv., OF 96-0486*.

Herbelin, A. L., and J. C. Westall (1999), FITEQL, A computer program for determination of chemical equilibrium constants from experimental data, Version 4.0, *Rep. 99-01*, Chem. Dep., Oreg. State Univ., Corvallis.

Hsi, C. D., and D. Langmuir (1985), Adsorption of uranyl onto ferric oxyhydroxides; application of the surface complexation site-binding model, *Geochim. Cosmochim. Acta*, *49*(9), 1931–1941.

Kalmykov, S. N., and G. R. Choppin (2000), Mixed $Ca^{2+}/UO_2^{2+}/CO_3^{2-}$ complex formation at different ionic strengths, *Radiochim. Acta*, *88*, 603–606.

Kelly, S. D., M. G. Newville, L. Cheng, K. M. Kemner, S. R. Sutton, P. Fenter, N. C. Sturchio, and C. Spotl (2003), Uranyl incorporation in natural calcite, *Environ. Sci. Technol.*, *37*(7), 1284–1287.

Kent, D. B., R. H. Abrams, J. A. Davis, J. A. Coston, and D. R. LeBlanc (2000), Modeling the influence of variable pH on the transport of zinc in a contaminated aquifer using semiempirical surface complexation models, *Water Resour. Res.*, *36*(12), 3411–3425.

Kohler, M., G. P. Curtis, D. B. Kent, and J. A. Davis (1996), Experimental investigation and modeling of uranium(VI) transport under variable chemical conditions, *Water Resour. Res.*, *32*(12), 3539–3551.

Kohler, M., D. E. Meece, G. P. Curtis, and J. A. Davis (2004), Methods for estimating adsorbed uranium (VI) and distribution coefficients in contaminated sediments, *Environ. Sci. Technol.*, *38*(1), 240–247.

Langmuir, D. (1997), *Aqueous Environmental Geochemistry*, Prentice-Hall, Upper Saddle River, N. J.

Lee, R. W., S. A. Jones, E. L. Kuniansky, G. Harvey, B. S. Lollar, and G. F. Slater (2000), Phreatophyte influence on reductive dechlorination in a shallow aquifer contaminated with trichloroethene (TCE), *Int. J. Phytoremediation*, *2*(3), 193–211.

McKinley, J. P., J. M. Zachara, S. C. Smith, and G. D. Turner (1995), The influence of uranyl hydrolysis and multiple site-binding reactions on adsorption of U(VI) to montmorillonite, *Clays Clay Miner.*, *43*(5), 586–598.

Pabalan, R. T., D. R. Turner, F. P. Bertetti, and J. D. Prikryl (1998), $Uranium^{VI}$ sorption onto selected mineral surfaces; key geochemical parameters, in *Adsorption of Metals by Geomedia; Variables, Mechanisms, and Model Applications*, edited by E. A. Jenne, pp. 99–130, Elsevier, New York.

Parkhurst, D. L., K. G. Stollenwerk, and J. A. Colman (2003), Reactive-transport simulation of phosphorus in the sewage plume at the Massachusetts Military Reservation, *U.S. Geol. Surv. Water Resour. Invest. Rep., 03-401799-4259*.

Poeter, E. P., and M. C. Hill (1998), UCODE, a computer code for universal inverse modeling, *U.S. Geol. Surv. Water Resour. Invest., 98-4080*.

Pollock, D. W. (1994), User's guide for MODPATH/MODPATH-PLOT, Version 3: A particle tracking post-processing package for MODFLOW, the U.S. Geological Survey finite-difference ground-water flow model, *U.S. Geol. Surv. Open File Rep., 94-464*.

Portniaguine, O., and D. K. Solomon (1998), Parameter estimation using groundwater age and head data, Cape Cod, Massachusetts, *Water Resour. Res.*, *34*(4), 637–645.

Prikryl, J. D., A. Jain, D. R. Turner, and R. T. Pabalan (2001), Uranium$^{(VI)}$ sorption behavior on silicate mineral mixtures, *J. Contam. Hydrol.*, *47*(2–4), 241–253.

Reardon, E. J. (1981), Kd's—Can they be used to describe reversible ion sorption reactions in contaminant migration?, *Ground Water*, *19*(3), 279–286.

Reeder, R. J., M. Nugen, D. D. Tait, D. E. Morris, S. M. Heald, K. M. Beck, W. P. Hess, and A. Lanzirotti (2001), Coprecipitation of uranium (VI) with calcite: XAFS, micro-XAFS, and luminescence characterization, *Geochim. Cosmochim. Acta*, *65*(20), 3491–3503.

Reilly, T. E., N. L. Plummer, P. J. Phillips, and E. Busenberg (1994), The use of simulation and multiple environmental tracers to quantify groundwater flow in a shallow aquifer, *Water Resour. Res.*, *30*(2), 421–434.

Solomon, D. K., and P. G. Cook (2000), ^{3}H and ^{3}He, in *Environmental Tracers in Subsurface Hydrology*, edited by P. Cook and A. L. Herczeg, chap. 13, 529 pp., Springer, New York.

Stollenwerk, K. G. (1998), Molybdate transport in a chemically complex aquifer; field measurements compared with solute-transport model predictions, *Water Resour. Res.*, *34*(10), 2727–2740.

Tiedeman, C. R., D. M. Ely, M. C. Hill, and G. M. O'Brien (2004), A method for evaluating the importance of system state observations to model predictions, with application to the Death Valley regional groundwater flow system, *Water Resour. Res.*, *40*, W12411, doi:10.1029/2004WR003313.

Turner, D. R., and S. A. Sassman (1996), Approaches to sorption modeling for high-level waste performance assessment, *J. Contam. Hydrol.*, *21*(1–4), 311–332.

U.S. Department of Energy (USDOE) (1996), Programmatic environmental impact statement for the Uranium Mill Tailings Remedial Action Ground Water Project, vol. 1, Grand Junction, Colo.

U.S. Department of Energy (USDOE) (1998), Remedial action plan for the inactive uranium processing site at Naturita, Colorado. Remedial action selection report: Attachment 2, geology report: Attachment 3, groundwater hydrology report: Attachment 4, supplemental information, *Rep. DOE/AL/62350-249*, Washington, D. C.

U.S. Department of Energy (USDOE) (2003), Energy Information Administration, Naturita Mill Site Montrose County, Colorado, Naturita Mill Site, Montrose County, Colorado, report, Washington, D.C., Jan. (Available at http://www.eia.doe.gov/cneaf/nuclear /page/umtra/naturita_title1.html)

Villalobos, M., M. A. Trotz, and J. O. Leckie (2001), Surface complexation modeling of carbonate effects on the adsorption of Cr (VI), Pb (II), and U(VI) on goethite, *Environ. Sci. Technol.*, *35*(19).

Waite, T. D., J. A. Davis, T. E. Payne, G. A. Waychunas, and N. Xu (1994), Uranium (VI) adsorption to ferrihydrite; application of a surface complexation model, *Geochim. Cosmochim. Acta*, *58*(24), 5465–5478.

Waite, T. D., J. A. Davis, B. R. Fenton, and T. E. Payne (2000), Approaches to modelling uranium(VI) adsorption on natural mineral assemblages, *Radiochim. Acta*, *88*(9/11), 687–699.

Wazne, M., G. P. Korfiatis, and X. Meng (2003), Carbonate effects on hexavalent uranium adsorption by iron oxyhydroxide, *Environ. Sci. Technol.*, *37*(16), 3619–3624.

Westall, J. C., M. Cernik, and M. Borkovec (1998), Modeling metal speciation in aquatic systems, in *Metals in Surface Water*, pp. 191–216, CRC Press, Boca Raton, Fla.

Zheng, C., and P. P. Wang (1999), MT3DMS, a modular three-dimensional multi-species transport model for simulation of advection, dispersion and chemical reactions of contaminants in groundwater systems; documentation and user's guide, *Contract Rep. SERDP-99-1*, 202 pp., U.S. Army Eng. Res. and Dev. Cent., Vicksburg, Miss.

Zhu, C. (2003), A case against K_d-based transport models; natural attenuation at a mill tailings site; reactive transport modeling in the geosciences, *Comput. Geosci.*, *29*(3), 351–359.

Zhu, C., and D. S. Burden (2001), Mineralogical compositions of aquifer matrix as necessary initial conditions in reactive contaminant transport models, *J. Contam. Hydrol.*, *51*(3–4), 145–161.

Zhu, C., F. Q. Hu, and D. S. Burden (2001), Multi-component reactive transport modeling of natural attenuation of an acid groundwater plume at a uranium mill tailings site, *J. Contam. Hydrol.*, *52*(1–4), 85–108.

G. P. Curtis, U.S. Geological Survey, 345 Middlefield Road, MS 409, Menlo Park, CA 94025, USA. (gpcurtis@usgs.gov)

J. A. Davis, U.S. Geological Survey, 345 Middlefield Road, MS 465, Menlo Park, CA 94025, USA. (jadavis@usgs.gov)

D. L. Naftz, U.S. Geological Survey, 2329 W. Orton Circle, West Valley City, UT 84119, USA. (dlnaftz@usgs.gov)